Forest of Gold Nanowires: A New Type of Nanocrystal Growth

Jiating He,[†,§] Yawen Wang,[†,§] Yuhua Feng,[†] Xiaoying Qi,[‡] Zhiyuan Zeng,[‡] Qing Liu,[‡] Wei Shan Teo,[†] Chee Lip Gan,[‡] Hua Zhang,[‡] and Hongyu Chen[†,*]

[†]Division of Chemistry and Biological Chemistry, Nanyang Technological University, Singapore 637371 and [‡]School of Materials Science and Engineering, Nanyang Technological University, Singapore 639798. §These authors contributed equally to this work.

ABSTRACT We report a nanowire growth that is highly unconventional: (1) nanowires can grow from substrate-bound seeds but cannot from colloidal seeds under otherwise the same conditions; (2) the nanowires grow from only one side of the seeds, with their diameter independent of the size of the seeds; and (3) vertically aligned ultrathin nanowires are obtained on substrates, using aqueous solution and ambient conditions. With carefully designed experiments, we propose and test a new mechanism that can explain these unusual phenonmena. It turns out that the strong binding of ligands in this system forces selective deposition of Au at the ligand-deficient interface between Au seeds and oxide substrates. This means of promoting anisotropic growth of nanocrystals into nanowires is previously unknown in the literature. We are able to pinpoint the site of active growth and explain the control of nanowire width. The sustained growth at the active site and the inhibited growth at its parameter push the nanocrystals upward into wires; their diameter is dependent on the dynamic competition of the two processes. The site-specific growth from substrate-anchored seeds provides a rare means to create substrate-nanowire hierarchical structures in aqueous solution under ambient conditions. Rendering a surface conductive, particularly one with complex surface morphology, is now made easy.

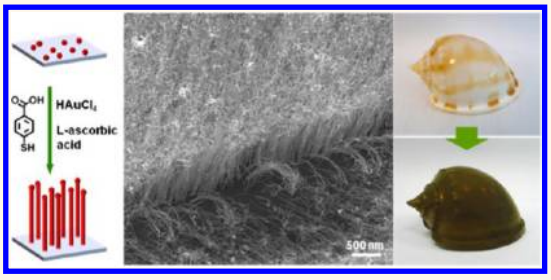

KEYWORDS: nanowire · anisotropic growth · substrate-bound seeds · ligand control · active site · hierarchical structure

Controlling where and how nanocrystals grow is of fundamental importance for nanoscience and nanotechnology. In solution, such control is often realized by exploiting the facet-specific binding of surface ligands, so that preferred growth of certain facets determines the shape of nanocrystals.[1−3] Because of the intrinsic symmetry of crystal lattice, a nanocrystal always has multiple equivalent facets. Without a reason, they should grow equivalently.

Nanowire (NW) is a special type of nanocrystal with extremely large anisotropy.[2−11] Any NW must have started as a small primary nucleus with multiple equivalent facets, before transitioning to an anisotropic growth mode. Thus, a prominent question is why the two ends of a wire grow so much faster than the rest of the equivalent facets. It cannot be solely explained by the difference in the binding affinity of ligands. Thus, additional factors have been proposed in the literature: (a) cylindrical surfactant micelles such as those of oleylamine can serve as a structural template;[12−16] (b) the 5-fold twinning defects in pentagonal NWs can induce sufficient strain to restrict their lateral growth;[17−20] (c) the screw-dislocation on a facet can promote its rapid growth causing large anisotropy in the resulting NWs;[21−23] and (d) during the oriented attachment of semiconductor nanocrystals, their dipole interactions can lead to linear growth of NWs.[24−26] In addition, in the vapor−liquid−solid (VLS) growth under high temperature, the molten seeds confine the cross-sectional width of the nanocrystal, catalyzing its linear growth.[27−31] In contrast to these known systems, we now present a new origin for the anisotropy in NW growth.

In the conventional growth of metal NWs in solution, there are several common characteristics: The known surface ligands are all weakly binding, including oleylamine,[12−15,32,33] hexadecyltrimethylammonium bromide (CTAB),[7,34−36] polyvinylpyrrolidone (PVP),[5,17,19,20,37−39] and their analogues.[40,41] On the other hand, seeded growth of NWs was rarely reported,[16,18,34] particularly for ultrathin metal NWs ($d < 10$ nm). Without seeds, the known factors above for

* Address correspondence to hongyuchen@ntu.edu.sg.

Received for review January 14, 2013 and accepted February 26, 2013.

Published online 10.1021/nn4001885

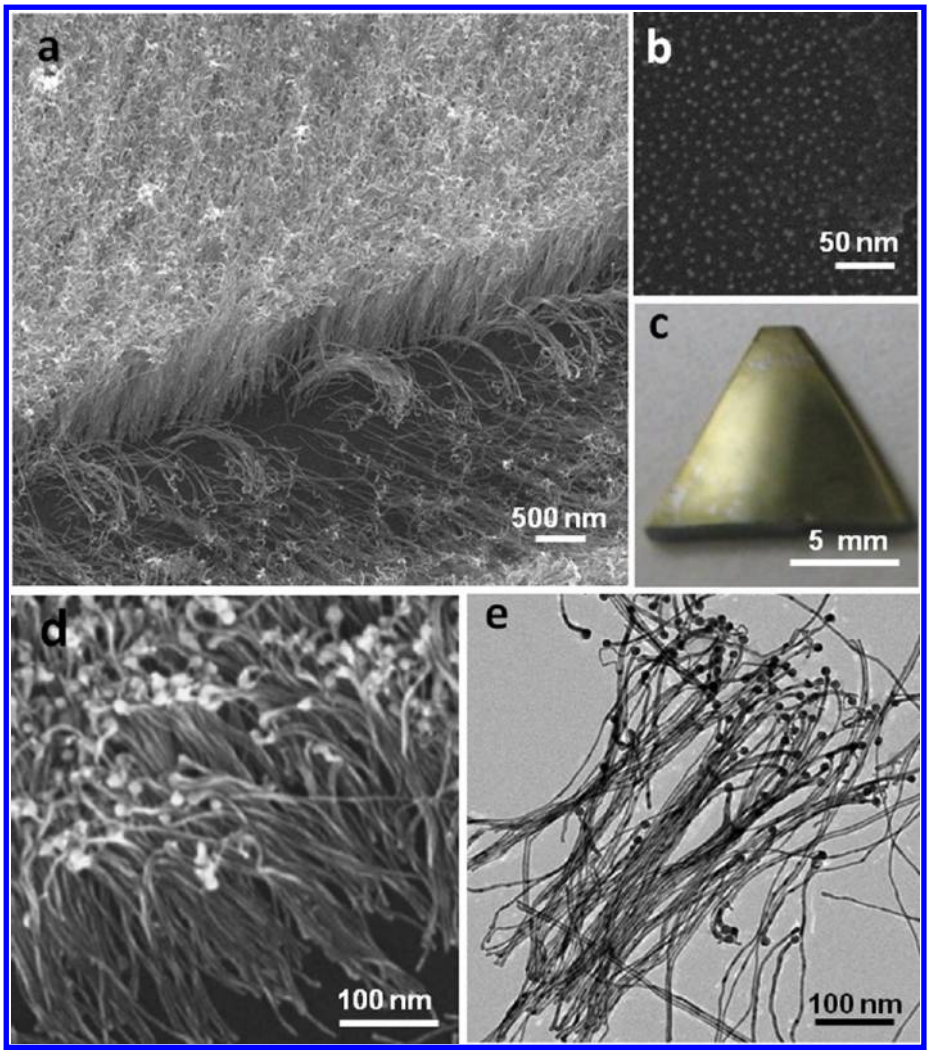

Figure 1. (a,b) SEM image of (a) vertically aligned AuNWs on a Si/SiO_2 substrate, (b) Au seeds (d = 3−5 nm) adsorbed on the substrate; (c) A photograph of the resulting Si wafer in sample a; (d) SEM image of AuNWs synthesized using 15 nm AuNPs as seeds; (e) TEM image of the AuNWs scratched from sample d.

inducing anisotropic nanocrystal growth cannot be easily applied to a substrate. This is probably the reason why solution growth of anchored NWs on a substrate has so far not been demonstrated.

Here, we report a new type of NW growth in polar solution under ambient conditions. By using a strong-binding ligand, 4-mercaptobenzoic acid (MBA), Au seeds anchored on oxide substrates can "catalyze" the growth of vertically aligned ultrathin AuNWs (d = 6 nm, Figure 1a). The growth mode is similar in appearance to the VLS growth in chemical vapor deposition, but the underlying mechanism is radically different. The strong ligand is of critical importance, but not because it has affinity to any special facet: Au can be continuously deposited at the Au-substrate interface because ligands cannot effectively bind there, whereas the instant binding of strong ligands inhibits the growth at the perimeter of this active site, pushing the nanocrystals upward into anisotropic NWs (Figure 2b). Under this unique growth mode, the diameter of the resulting NWs is, surprisingly, independent of the size of the seeds, but dependent on the relative deposition rates of Au and ligands. We further identify the location of active growth and thus prove the presence of a single active site per each NW.

RESULTS AND DISCUSSION

Chips of Si wafer were used as substrates for growing AuNWs. The top thermal oxide layer of the wafer was functionalized with amino groups using 3-aminopropyltriethoxysilane (APTES) to facilitate the subsequent adsorption of citrate-stabilized Au seeds (d = 3−5 nm).[42−46] After adsorbing Au seeds (Figure 1b), the substrate was immersed in a water/ethanol (v/v = 3:1) solution containing ligand MBA (550 μM), $HAuCl_4$ (1.7 mM), and reducing agent L-ascorbic acid (4.1 mM). After 15 min, the substrate was retrieved, rinsed with water, and then dried. The gilding of the substrate surface confirmed Au deposition (Figure 1c). As revealed by scanning electron microscopy (SEM), the wafer surface was

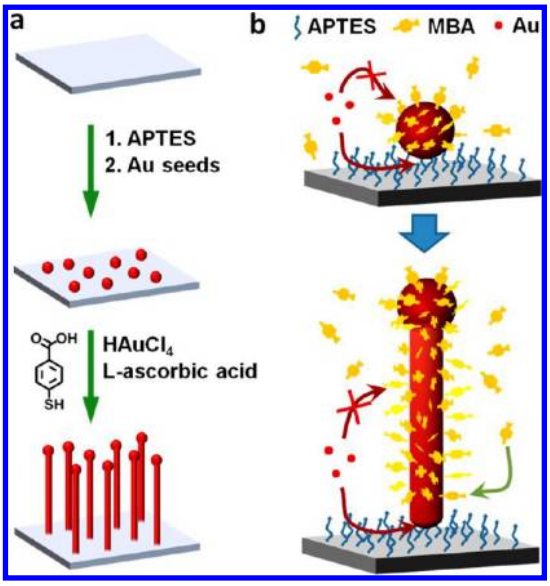

Figure 2. (a,b) Schematics illustrating (a) the specific conditions used for the syntheses of AuNWs on Si/SiO_2 substrates; (b) because of the strong ligands, the Au deposition selectively occur at the Au−substrate interface.

covered with a dense layer of vertically aligned AuNWs. At the edge of a scratch mark (Figure 1a), it can be clearly observed that the AuNWs were over 1 μm in length, with uniform width and height. Such length is remarkable considering the short 15 min growth. Though these AuNWs were roughly parallel to each other, they were not perfectly straight, unlike the typical single-crystalline NWs.[6] Despite the complex hierarchical structure, the synthesis was facile and reproducible. The method only involved the mixing of a few solutions in correct ratio and then treating the seed-adsorbed substrate at room temperature. It can be easily scaled up without significant change in the resulting nanostructures.

Unlike the typical solution methods for growing NWs,[4−8,17,19,20] in our system the NWs cannot grow without the substrate: when free Au seeds (3−5 nm) were used without being adsorbed to the Si/SiO_2 substrate, the seeds simply grew larger with nearly spherical shape, but NWs were not formed.[47] Hence, it appeared that the adsorption of the seeds on the silica surface was essential. We must identify the anisotropic factor that is responsible for shifting the near-spherical growth mode to the NW growth. The presence of the substrate in itself was clearly insufficient in this role.

The width of the AuNWs was found to be independent of the size of the seeds. When large 15 nm AuNPs were used, they ended up on the top of the resulting thin AuNWs (Figure 1d). Obviously, the formation of the AuNWs has caused the 15 nm seeds to be elevated from the substrate. Therefore, the initial Au deposition must have occurred at the Au−silica interface. After these AuNWs were scratched off and characterized by transmission electron microscopy (TEM), the diameter was measured as 6 nm (Figure 1e), the same as those prepared from smaller seeds. There was no obvious increase in the size of the 15 nm seeds, which roughly retained their spherical shape. It was surprising that each AuNW was grown from a Au seed but its diameter was much smaller.[48,49] Normally, in colloidal synthesis the seeds are the heterogeneous nucleation centers; the nanocrystals grown around them are usually larger.[1] In solid-state growth such as *via* the VLS mechanism, the entire molten seed is the catalyst, making it hard to grow smaller structures.[27]

We found that the width of AuNWs was dependent on the ligand concentration. When the MBA concentration was decreased from 550 to 55 and 28 μM, the resulting nanostructures became teeth-like with shorter AuNWs. However, their average diameter increased from 6 to 13, and then 17 nm (Figure 3a−c). Upon further decrease of the ligand concentration to 5.5 μM, Au deposition on the seeds formed an overcoating layer (*i.e.*, near-spherical growth mode) without any sign of NW formation (Figure 3d).

Study of the AuNWs by high-resolution TEM (HRTEM) showed that they were polycrystalline with frequent occurrence of *random* twinning defects (Figure 4a). Hence, the unidirectional growth of AuNWs was not consistent with screw-dislocation driven growth, which is an orderly process.[11,21−23] Occasionally, single-crystalline segments can also be observed, as illustrated by the Fourier transform analysis of a local section (Figure 4b and inset). The AuNWs were cut by focus ion beam (FIB) to reveal their cross sections, which were circular in all of the observed cases (Figure 4c).[47] There was no preferred surface facet that we could identify. Thus, these AuNWs with nonspecific surface facets were distinctively different from those synthesized in the presence of oleylamine and CTAB, whose side surfaces were bound with specific facets.[6,34,50,51] In this aspect, the NW growth is different from the conventional growth models.

After the initial Au deposition at the seed-substrate interface, it is essential to understand if the subsequent growth occurred at the top seed−AuNW interface or the bottom AuNW−substrate interface. We can devise the reaction conditions to distinguish the temporal evolution of the AuNWs. To clearly observe the width control, 5 nm Au seeds were used. The substrate was first grown in 550 μM of MBA, and then rapidly transferred without drying to a solution of 28 μM of MBA. The resulting AuNWs had thin heads and thick tails (Figure 3e). Conversely, when the growth was carried out first with low and then with high ligand concentration, the resulting AuNWs had thick heads and thin tails (Figure 3g). Therefore, the Au growth must have occurred at the Au−substrate interface after the seed was elevated from the substrate. This is clearly different from the VLS mechanism, where the materials

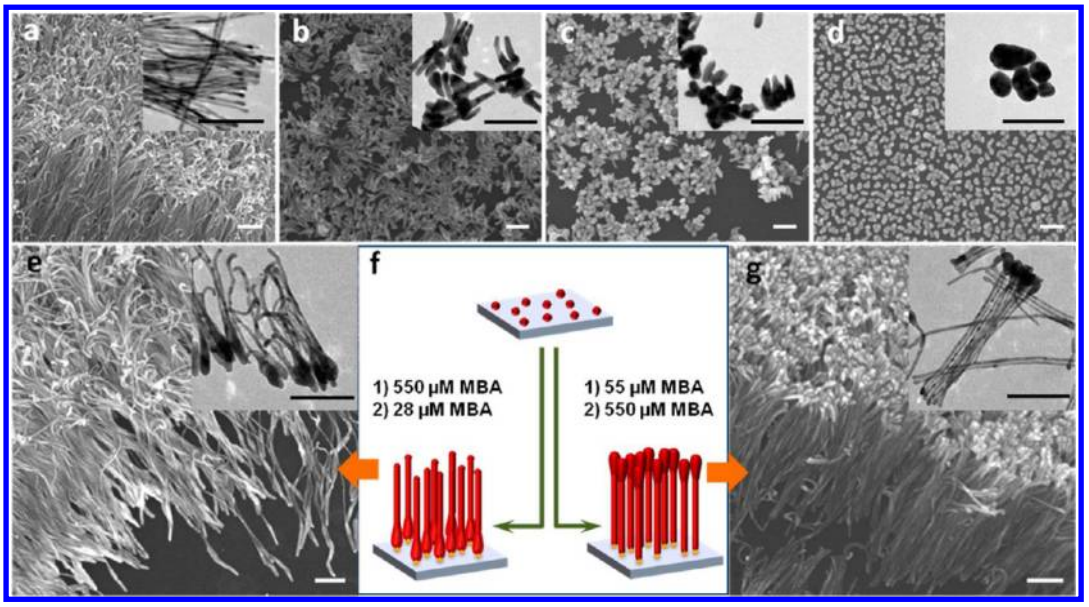

Figure 3. (a−e) SEM and TEM (shown in the insets) images of the AuNWs grown on Si/SiO_2 substrates at different ligand concentrations: (a) 550 μM, (b) 55 μM, (c) 28 μM, (d) 5.5 μM of MBA, and (e) the AuNWs grown first in 550 μM MBA solution for 5 min and then in 28 μM MBA solution for 5 min. (f) Schematics illustrating the specific conditions used in the syntheses of the AuNWs as shown in panels e and g, yellow stars indicate the active site of growth; (g) SEM and TEM images of the AuNWs grown first in 55 μM MBA solution and then in 550 μM MBA solution. All experiments were carried out using 5 nm Au seeds, so that the width control can be clearly observed. All scale bars = 100 nm.

deposition selectively occurs at the interface between the NWs and the molten seeds.[27]

Figure 3e provides additional evidence that Au deposition did not occur on the ligand covered surface. It appeared that once the thin sections were formed, they cannot grow thicker even when the ligand concentration was reduced during the second growth stage. This was probably because the densely packed ligand molecules on their surface cannot easily dissociate. This result was consistent with the absence of seed growth in Figure 1d,e.

In contrast to the absence of lateral growth, the continued longitudinal growth at the Au-substrate interface was obviously promoted by an anisotropic factor. Probably, it was because of insufficient ligand coverage at this interface (Figure 2b). Hence, the uniqueness of the "active" AuNW−substrate interface lies in its confined environment, which restricts ligand coordination and allows continued Au deposition. Because the ligand MBA binds strongly to Au,[52−55] its instant absorption inhibits Au deposition at the perimeter of the active site, inducing anisotropic growth and forcing the nanocrystals to be pushed upward. This model also explains why the AuNWs can be randomly polycrystalline but have a circular cross-section with uniform diameter. Without specific surface facets or internal lattice order, it is normally inconceivable how the polycrystalline domains with different lattice orientation would be able to coordinate with each other to form the orderly shape of wires.

The partial activation of the seed surface cannot easily occur: When free colloidal Au seeds were used, their surface facets were equivalently blocked by the ligand (*vide supra*).[47] Even when the seeds were anchored on a substrate, if the ligand concentration was too low, the insufficient ligand density on the seeds caused them to grow near-isotropically into larger spheres (Figure 3d).

Following this theory, the control of AuNW width (Figure 3a−c) can be interpreted as the effectiveness in switching off the lateral growth at the active site. In doing so, the rate at which the fresh AuNW is being generated from the active site must also be of importance. If ligand coordination cannot keep up with the new AuNW section being pushed upward, the AuNW must be able grow thicker. The increase in the length of AuNW (dL) should be proportional to the amount of Au deposition and inversely proportional to the cross-section of the AuNWs. Hence,

$$\mathrm{d}L = \frac{\mu \mathrm{d}t M}{\rho} \frac{4}{\pi D^2} \qquad (1)$$

where μ is the Au deposition rate, t is time, M and ρ are the molar mass and density of Au, and D is the diameter of the NW. On the other hand, the ligand coverage on the newly formed AuNW section must be able to keep up with the growth:

$$\mathrm{d}L = \frac{\gamma \mathrm{d}t}{k} \cdot \frac{1}{\pi D} \qquad (2)$$

where γ is the ligand diffusion rate and k is the ligand density on NW surface. Combining eq 1 and 2 gives

$$D = \frac{4Mk}{\rho} \frac{\mu}{\gamma} = a \frac{\mu}{\gamma} \qquad (3)$$

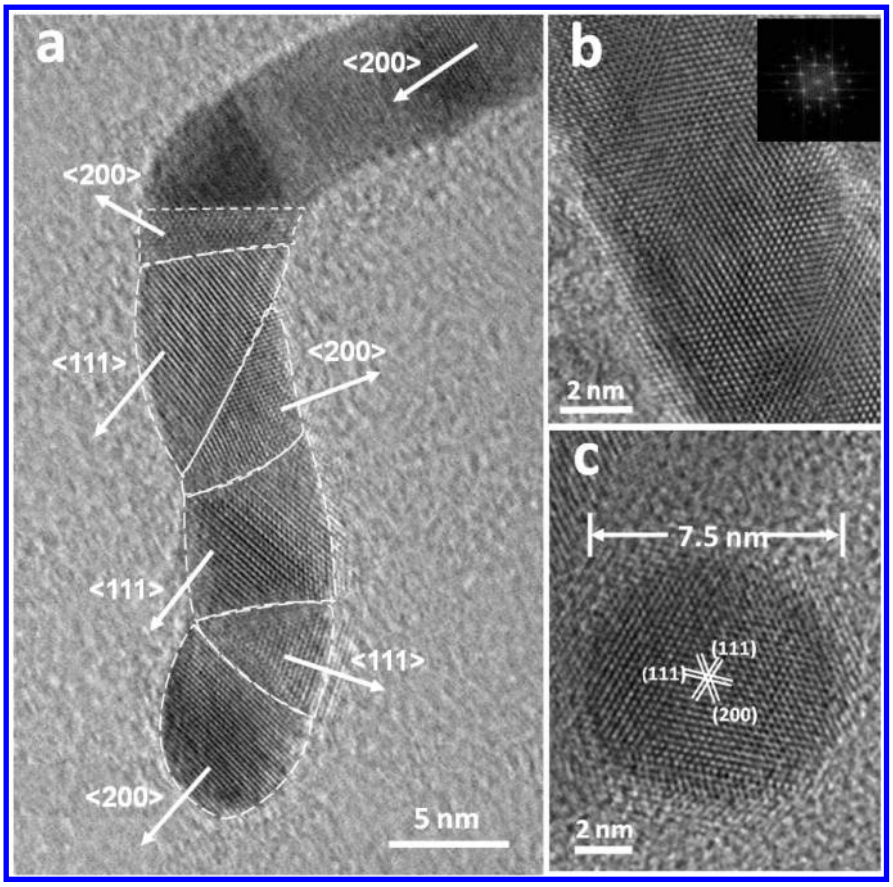

Figure 4. HRTEM images of (a) the substrate end of a typical ultrathin AuNW, (b) a single-crystalline segment (inset: Fourier transform pattern along the [011] zone axis), (c) a typical cross-section of a AuNW, prepared by FIB (see more examples in the Supporting Information).

where a is a constant. Hence, D is proportional to μ and inversely proportional to γ. Because of the complex environment of the Au−silica interface, further analysis of μ is not possible. Nevertheless, the trends are clear: faster ligand diffusion toward the active site should lead to thinner AuNWs; whereas faster Au deposition should lead to thicker AuNWs. Hence, the polycrystalline nature of the domains is not an issue in this unique growth mode. Given the homogeneous solution environment, the diffusion rates around the seeds or AuNWs should be similar and thus, the highly uniform diameter among the individual NWs can be explained.

Keeping all other conditions unchanged, lower ligand concentration should give a lower ligand diffusion rate. As shown in Figure 3a−d, AuNWs with larger diameter were obtained, consistent with eq 3. To further test our proposal, we modulated the rate of Au deposition by adjusting the concentration of $HAuCl_4$ and L-ascorbic acid: At the same ligand concentration, faster Au deposition led to thicker AuNW sections, whereas slower deposition led to thinner ones.[47] The resulting AuNWs were similar to those in Figure 3e,g.

Our results also ruled out that the ligand MBA might form templating cylindrical micelles: At a constant ligand concentration, the diameter of the presumed micelles should not change. Thus, by only changing the rate of Au deposition, the diameter of the resulting AuNWs should have remained constant. However, this speculation is inconsistent with the observations.[47]

Therefore, these results support a dynamic competition between Au deposition and ligand binding. Changing the rate of one process can tilt the balance of this competition, causing the width of the AuNWs to be adjusted. With this understanding, it is obvious that under our unique growth mode the AuNWs can grow thinner than the original seeds. It is also easy to recognize that the initial contact area of the seeds with the substrate is not of importance, because the width of AuNWs can be quickly adjusted during their growth. This is supported by the fact that the thick AuNW sections can be simply grown from the thin ones and *vice versa* (Figure 3e,g).

Under ambient conditions, we can now achieve seeded growth on a substrate, mimicking the popular VLS growth mode but with a drastically different mechanism: In the VLS growth, the growth material is first dissolved in the molten seed and subsequently nucleates onto the wire at the seed−wire interface.[27] The fact that the growth matierals are supplied to the molten seed means that the newly grown segment is always next to the seed. In our method, the growth

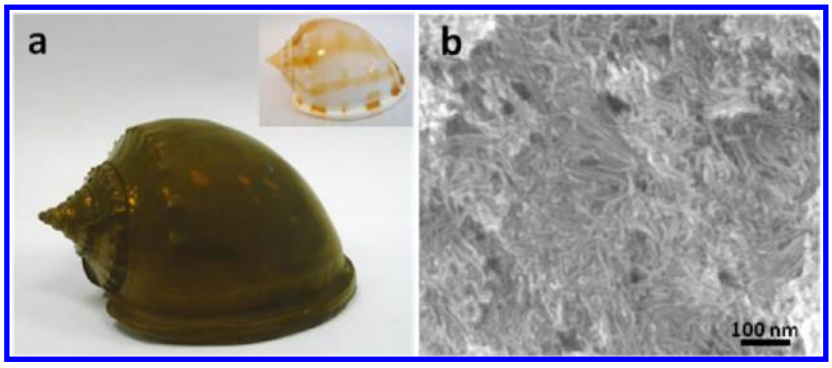

Figure 5. (a) Photographs of a trumpet shell before (inset) and after coating a AuNW film; (b) SEM image of AuNWs on sample a (a small chip was removed for characterization).

material is supplied to the active Au-substrate interface and, hence, the newly grown segment is always next to the substrate (Figure 3). Under the VLS mechanism, the size of the wire is highly dependent on the size of the seed and the surface ligands (if any) should have no effect on the nucleation event inside the molten droplet. Our new growth mechanism does not require molten seeds and thus allows ambient growth conditions. Moreover, the size of the growing wire is independent of the size of the seed. Instead, the size of the wire depends on how fast the ligands shut off the lateral growth and how fast Au is being supplied to the growth site eq 3.

The facile synthesis of substrate-anchored AuNWs can be easily extended to other oxide substrate such as glass, generating a uniform conductive film.[47] By simple immersion in a solution, this method can be easily applied to substrates with complex surface morphology such as a trumpet shell (Figure 5), making its surface conductive.[47] This feat is difficult to achieve by traditional methods such as spin-coating or doctor-blading.

CONCLUSIONS

We discovered a novel type of nanowire growth and proposed a new mechanism. The anisotropic growth of the nanocrystals was a consequence of both the strong surface ligands and the ligand-deficient interface between Au and substrate. To the best of our knowledge, this anisotrpic factor has not been previously known in the literature. The unique ability to create a nanowire–substrate hierarchical structure by solution methods opens windows for new synthetic strategies and mechanistic insights. The surface-adsorbed ultrathin nanowires are of importance for catalysis, conductive film, and nanoelectronic devices.

MATERIALS AND METHODS

Materials. All solutions were prepared using deionized water (resistivity >18 MΩ · cm^{-1}). 4-Mercaptobenzoic acid (MBA, 90%, Sigma Aldrich), hydrogen tetrachloroaurate(III) ($HAuCl_4$, 99.9%, Au 49% on metals basis, Alfa Aesar), trimethyl(methylcyclopentadienyl)platinum(IV) (98%, Sigma Aldrich), 3-aminopropyltriethoxysilane (APTES, Sigma Aldrich), sodium citrate tribasic dihydrate (99.0%, Sigma Aldrich), L-ascorbic acid (Sigma Aldrich) and ethanol (analytical grade) were used as received. Copper specimen grids (200 mesh) with Formvar/carbon support film (referred to as TEM grids in the text) were purchased from Beijing XXBR Technology, Co.

Characterization. Transmission electron microscopy (TEM) images were collected on a JEM-1400 (JEOL) operated at 100–120 kV. Field emission scanning electron microscopy (SEM) images were collected on a JEOL JSM-6700F. High-resolution TEM (HRTEM) images were taken from JEOL 2100 F field emission transmission electron microscopy operated at 200 kV.

Preparation of TEM Samples. TEM grids were treated with oxygen plasma in a Harrick plasma cleaner/sterilizer for 45 s to improve the surface hydrophilicity. The hydrophilic face of the TEM grid was then placed in contact with the sample solution. A filter paper was used to wick off the excess solution on the TEM grid, which was then dried in air for 30 min.

Synthesis of AuNWs on Si/SiO_2 Substrate. To prepare the vertical AuNWs on a Si/SiO_2 wafer, a Si wafer (about 0.6 cm^2) was pretreated with O_2 plasma for 10 min to improve its surface hydrophilicity. The wafer was then functionalized with an amino group by reacting with APTES solution (5 mM) for 1 h.[46] Subsequently, the wafer was soaked in excess citrate-stabilized Au seeds (3–5 nm) solution for 2 h to ensure the adsorption of Au seeds and rinsed with water twice to remove the excess Au seeds. The seeds-adsorbed wafer was then immersed in a reaction solution containing the ligand MBA (550 μM), $HAuCl_4$ (1.7 mM), and L-ascorbic acid (4.1 mM) for 15 min. Finally, the wafer was rinsed with ethanol and dried in air. The SEM image of the product was shown in Figure 1a. The generation of a thin conductive film on Si/SiO_2 wafer is similar to that of vertical AuNWs. All reaction conditions were unchanged except that the substrate was first functionalized with an amino group by reacting with lower APTES solution (10 μM) for 0.5 h.

For preparing AuNWs with 15 nm AuNPs as seeds (Figure 1d,e), all reaction conditions were unchanged except that citrate-stabilized AuNPs with a diameter of 15 nm were used as seeds[56,57] during the incubation with the amino-functionalized Si wafer.

To investigate the concentration-dependent growth of AuNWs, two sets of experiments were carried out: (a) Varying the ligand concentration. For the preparation of AuNWs or spherical NPs on Si/SiO_2 (Figure 3b–d), all reaction conditions were unchanged except that the concentration of MBA was lowered to 55 μM, 28 μM, and 5.5 μM, respectively; (b) Varying the concentration of $HAuCl_4$ and L-ascorbic acid (their relative ratio was kept unchanged). For the preparation of AuNWs or spherical NPs on Si/SiO_2 (Supporting Information, Figure S4a–c), all reaction conditions were unchanged except that the concentration of $HAuCl_4$ and L-ascorbic acid was lowered to (a) 0.6 mM and 1.4 mM, (b) 1.7 mM and 4.1 mM, and (c) 8.6 mM and 20.7 mM, respectively.

To identify the site of AuNW growth, a two-stage reaction was carried out. The substrate was first grown in a solution of 550 μM MBA for 5 min, and then rapidly transferred without drying to a solution of 28 μM MBA and grown for another 5 min. The concentrations of $HAuCl_4$ (1.7 mM) and L-ascorbic acid (4.1 mM) were constant in both stages. The resulting AuNWs had thin heads and thick tails (Figure 3e). Conversely, when the growth was carried out first with a low concentration of MBA (55 μM) and then with a high concentration (550 μM), the resulting AuNWs had thick heads and thin tails (Figure 3g). This phenomenon was also observed by changing the concentrations of $HAuCl_4$ and L-ascorbic acid with fixed ligand concentration as shown in Supporting Information, Figure S4d,e.

Generation of a Uniform Conductive Film on Trumpet Shell. The generation of a uniform conductive film is similar to that of vertical AuNWs on Si/SiO_2 wafer. When a trumpet shell was used as substrate, it was first functionalized with an amino group by reacting with APTES solution (5 mM) for 0.5 h. Subsequently, the shell was soaked in excess citrate-stabilized Au seeds (3−5 nm) solution for 1 h, and rinsed twice with water to remove the excess Au seeds. The seeds-adsorbed shell was then put into an ethanol solution containing the ligand MBA (30 mM), $HAuCl_4$ (100 mM), and L-ascorbic acid (260 mM) for 30 min. The SEM image of the AuNWs on the trumpet shell (a small chip was removed for characterization) is shown in Figure 5b and Supporting Information, Figure S5.

Preparation of AuNW Cross-Section. The cross sections of AuNWs were prepared by using FEI Novatech Nanolab DualBeam 600i, combining ultrahigh resolution field emission scanning electron microscopy (SEM) and precise focused ion beam (FIB) and deposition. First, the Si wafer with AuNWs lying on its surface was properly loaded into the FIB chamber. Protective deposition of a Pt layer to the area of interest was applied by using electron beam induced deposition to protect the AuNW from ion beam damage during subsequent milling. The electron beam (5 kV and 0.4 nA) for protective deposition is not strong enough to fully dissociate the precursor trimethyl(methylcyclopentadienyl)platinum(IV), so this protective layer is in amorphous state, containing a considerable amount of coordination compounds from the precursor. Then a thin lamellar for TEM characterization was cut out by FIB milling. Finally, low energy cleaning was carried out to remove the amorphous layer on the cut surface.

Conflict of Interest: The authors declare no competing financial interest.

Acknowledgment. The authors are grateful for financial support from the MOE (ARC 13/09) and NRF (CRP-4-2008-06) of Singapore.

Supporting Information Available: Large-area views of TEM, SEM, and HRTEM images; a photograph of conductivity test on the nanowire-coated trumpet shell. This material is available free of charge *via* the Internet at http://pubs.acs.org.

REFERENCES AND NOTES

1. Habas, S. E.; Lee, H.; Radmilovic, V.; Somorjai, G. A.; Yang, P. Shaping Binary Metal Nanocrystals through Epitaxial Seeded Growth. *Nat. Mater.* **2007**, *6*, 692–697.
2. Cademartiri, L.; Ozin, G. A. Ultrathin Nanowires—a Materials Chemistry Perspective. *Adv. Mater.* **2009**, *21*, 1013–1020.
3. Xia, Y.; Xiong, Y. J.; Lim, B.; Skrabalak, S. E. Shape-Controlled Synthesis of Metal Nanocrystals: Simple Chemistry Meets Complex Physics? *Angew. Chem., Int. Ed.* **2009**, *48*, 60–103.
4. Lee, E. P.; Chen, J.; Yin, Y.; Campbell, C. T.; Xia, Y. Pd-Catalyzed Growth of Pt Nanoparticles or Nanowires as Dense Coatings on Polymeric and Ceramic Particulate Supports. *Adv. Mater.* **2006**, *18*, 3271–3274.
5. Lee, J.-Y.; Connor, S. T.; Cui, Y.; Peumans, P. Solution-Processed Metal Nanowire Mesh Transparent Electrodes. *Nano Lett.* **2008**, *8*, 689–692.
6. Wang, C.; Sun, S. Facile Synthesis of Ultrathin and Single-Crystalline Au Nanowires. *Chem. Asian. J.* **2009**, *4*, 1028–1034.
7. Critchley, K.; Khanal, B. P.; Górzny, M. Ł.; Vigderman, L.; Evans, S. D.; Zubarev, E. R.; Kotov, N. A. Near-Bulk Conductivity of Gold Nanowires as Nanoscale Interconnects and the Role of Atomically Smooth Interface. *Adv. Mater.* **2010**, *22*, 2338–2342.
8. Wu, H.; Hu, L. B.; Rowell, M. W.; Kong, D. S.; Cha, J. J.; McDonough, J. R.; Zhu, J.; Yang, Y. A.; McGehee, M. D.; Cui, Y. Electrospun Metal Nanofiber Webs as High-Performance Transparent Electrode. *Nano Lett.* **2010**, *10*, 4242–4248.
9. Kim, C.-H.; Cha, S.-H.; Kim, S. C.; Song, M.; Lee, J.; Shin, W. S.; Moon, S.-J.; Bahng, J. H.; Kotov, N. A.; Jin, S.-H. Silver Nanowire Embedded in P3HT/PCBM for High-Efficiency Hybrid Photovoltaic Device Applications. *ACS Nano* **2011**, *5*, 3319–3325.
10. Garnett, E. C.; Cai, W. S.; Cha, J. J.; Mahmood, F.; Connor, S. T.; Christoforo, M. G.; Cui, Y.; McGehee, M. D.; Brongersma, M. L. Self-Limited Plasmonic Welding of Silver Nanowire Junctions. *Nat. Mater.* **2012**, *11*, 241–249.
11. Jin, S.; Bierman, M. J.; Morin, S. A. A New Twist on Nanowire Formation: Screw-Dislocation-Driven Growth of Nanowires and Nanotubes. *J. Phys. Chem. Lett.* **2010**, *1*, 1472–1480.
12. Huo, Z.; Tsung, C.-k.; Huang, W.; Zhang, X.; Yang, P. Sub-Two Nanometer Single Crystal Au Nanowires. *Nano Lett.* **2008**, *8*, 2041–2044.
13. Wang, C.; Hu, Y.; Lieber, C. M.; Sun, S. Ultrathin Au Nanowires and Their Transport Properties. *J. Am. Chem. Soc.* **2008**, *130*, 8902–8903.
14. Pazos-Pérez, N. s.; Baranov, D.; Irsen, S.; Hilgendorff, M.; Liz-Marzán, L. M.; Giersig, M. Synthesis of Flexible, Ultrathin Gold Nanowires in Organic Media. *Langmuir* **2008**, *24*, 9855–9860.
15. Lu, X.; Yavuz, M. S.; Tuan, H.-Y.; Korgel, B. A.; Xia, Y. Ultrathin Gold Nanowires Can Be Obtained by Reducing Polymeric Strands of Oleylamine−AuCl Complexes Formed *via* Aurophilic Interaction. *J. Am. Chem. Soc.* **2008**, *130*, 8900–8901.
16. Azulai, D.; Cohen, E.; Markovich, G. Seed Concentration Control of Metal Nanowire Diameter. *Nano Lett.* **2012**, *12*, 5552–5558.
17. Sun, Y. G.; Xia, Y. N. Large-Scale Synthesis of Uniform Silver Nanowires through a Soft, Self-Seeding, Polyol Process. *Adv. Mater.* **2002**, *14*, 833–837.
18. Sun, Y. G.; Yin, Y. D.; Mayers, B. T.; Herricks, T.; Xia, Y. N. Uniform Silver Nanowires Synthesis by Reducing $AgNO_3$ with Ethylene Glycol in the Presence of Seeds and Poly(vinyl pyrrolidone). *Chem. Mater.* **2002**, *14*, 4736–4745.
19. Sun, Y.; Mayers, B.; Herricks, T.; Xia, Y. Polyol Synthesis of Uniform Silver Nanowires: A Plausible Growth Mechanism and the Supporting Evidence. *Nano Lett.* **2003**, *3*, 955–960.
20. Hu, L.; Kim, H. S.; Lee, J.-Y.; Peumans, P.; Cui, Y. Scalable Coating and Properties of Transparent, Flexible, Silver Nanowire Electrodes. *ACS Nano* **2010**, *4*, 2955–2963.
21. Bierman, M. J.; Lau, Y. K. A.; Kvit, A. V.; Schmitt, A. L.; Jin, S. Dislocationdriven Nanowire Growth and Eshelby Twist. *Science* **2008**, *320*, 1060–1063.
22. Morin, S. A.; Bierman, M. J.; Tong, J.; Jin, S. Mechanism and Kinetics of Spontaneous Nanotube Growth Driven by Screw Dislocations. *Science* **2010**, *328*, 476–480.
23. Meng, F.; Jin, S. The Solution Growth of Copper Nanowires and Nanotubes Is Driven by Screw Dislocations. *Nano Lett.* **2012**, *12*, 234–239.
24. Tang, Z. Y.; Kotov, N. A.; Giersig, M. Spontaneous Organization of Single CdTe Nanoparticles into Luminescent Nanowires. *Science* **2002**, *297*, 237–240.
25. Pradhan, N.; Xu, H. F.; Peng, X. G. Colloidal CdSe Quantum Wires by Oriented Attachment. *Nano Lett.* **2006**, *6*, 720–724.
26. Patla, I.; Acharya, S.; Zeiri, L.; Israelachvili, J.; Efrima, S.; Golan, Y. Synthesis, Two-Dimensional Assembly, and Surface Pressure-Induced Coalescence of Ultranarrow PbS Nanowires. *Nano Lett.* **2007**, *7*, 1459–1462.
27. Law, M.; Goldberger, J.; Yang, P. D. Semiconductor Nanowires and Nanotubes. *Annu. Rev. Mater. Res.* **2004**, *34*, 83–122.

28. Gao, P. X.; Ding, Y.; Mai, W. J.; Hughes, W. L.; Lao, C. S.; Wang, Z. L. Conversion of Zinc Oxide Nanobelts into Superlattice-Structured Nanohelices. *Science* **2005**, *309*, 1700–1704.
29. Wang, X. J.; Li, G. P.; Chen, T.; Yang, M. X.; Zhang, Z.; Wu, T.; Chen, H. Y. Polymer-Encapsulated Gold-Nanoparticle Dimers: Facile Preparation and Catalytical Application in Guided Growth of Dimeric Zno-Nanowires. *Nano Lett.* **2008**, *8*, 2643–2647.
30. Zhang, Z.; Wong, L. M.; Ong, H. G.; Wang, X. J.; Wang, J. L.; Wang, S. J.; Chen, H.; Wu, T. Self-Assembled Shape- and Orientation-Controlled Synthesis of Nanoscale Cu_3Si Triangles, Squares, and Wires. *Nano Lett.* **2008**, *8*, 3205–3210.
31. Wu, Y. Y.; Yan, H. Q.; Huang, M.; Messer, B.; Song, J. H.; Yang, P. D. Inorganic Semiconductor Nanowires: Rational Growth, Assembly, and Novel Properties. *Chem.—Eur. J.* **2002**, *8*, 1261–1268.
32. Halder, A.; Ravishankar, N. Ultrafine Single-Crystalline Gold Nanowire Arrays by Oriented Attachment. *Adv. Mater.* **2007**, *19*, 1854–1858.
33. Feng, H.; Yang, Y.; You, Y.; Li, G.; Guo, J.; Yu, T.; Shen, Z.; Wu, T.; Xing, B. Simple and Rapid Synthesis of Ultrathin Gold Nanowires, Their Self-Assembly and Application in Surface-Enhanced Raman Scattering. *Chem. Commun.* **2009**, 1984–1986.
34. Kim, F.; Sohn, K.; Wu, J.; Huang, J. Chemical Synthesis of Gold Nanowires in Acidic Solutions. *J. Am. Chem. Soc.* **2008**, *130*, 14442–14443.
35. Krichevski, O.; Tirosh, E.; Markovich, G. Formation of Gold−Silver Nanowires in Thin Surfactant Solution Films. *Langmuir* **2006**, *22*, 867–870.
36. Krichevski, O.; Markovich, G. Growth of Colloidal Gold Nanostars and Nanowires Induced by Palladium Doping. *Langmuir* **2007**, *23*, 1496–1499.
37. Huang, X.; Zheng, N. One-Pot, High-Yield Synthesis of 5-Fold Twinned Pd Nanowires and Nanorods. *J. Am. Chem. Soc.* **2009**, *131*, 4602–4603.
38. Wang, Y.; Wang, Q.; Sun, H.; Zhang, W.; Chen, G.; Wang, Y.; Shen, X.; Han, Y.; Lu, X.; Chen, H. Chiral Transformation: From Single Nanowire to Double Helix. *J. Am. Chem. Soc.* **2011**, *133*, 20060–20063.
39. Tao, A.; Kim, F.; Hess, C.; Goldberger, J.; He, R. R.; Sun, Y. G.; Xia, Y. N.; Yang, P. D. Langmuir−Blodgett Silver Nanowire Monolayers for Molecular Sensing Using Surface-Enhanced Raman Spectroscopy. *Nano Lett.* **2003**, *3*, 1229–1233.
40. Imura, Y.; Tanuma, H.; Sugimoto, H.; Ito, R.; Hojo, S.; Endo, H.; Morita, C.; Kawai, T. Water-Dispersible Ultrathin Au Nanowires Prepared Using a Lamellar Template of a Long-Chain Amidoamine Derivative. *Chem. Commun.* **2011**, *47*, 6380–6382.
41. Hong, X.; Wang, D.; Yu, R.; Yan, H.; Sun, Y.; He, L.; Niu, Z.; Peng, Q.; Li, Y. Ultrathin Au−Ag Bimetallic Nanowires with Coulomb Blockade Effects. *Chem. Commun.* **2011**, *47*, 5160–5162.
42. Jackson, J. B.; Halas, N. J. Silver Nanoshells: Variations in Morphologies and Optical Properties. *J. Phys. Chem. B* **2001**, *105*, 2743–2746.
43. Pham, T.; Jackson, J. B.; Halas, N. J.; Lee, T. R. Preparation and Characterization of Gold Nanoshells Coated with Self-Assembled Monolayers. *Langmuir* **2002**, *18*, 4915–4920.
44. Prodan, E.; Radloff, C.; Halas, N. J.; Nordlander, P. A Hybridization Model for the Plasmon Response of Complex Nanostructures. *Science* **2003**, *302*, 419–422.
45. Hirsch, L. R.; Gobin, A. M.; Lowery, A. R.; Tam, F.; Drezek, R. A.; Halas, N. J.; West, J. L. Metal Nanoshells. *Ann. Biomed. Eng.* **2006**, *34*, 15–22.
46. Bardhan, R.; Mukherjee, S.; Mirin, N. A.; Levit, S. D.; Nordlander, P.; Halas, N. J. Nanosphere-in-a-Nanoshell: A Simple Nanomatryushka. *J. Phys. Chem. C* **2009**, *114*, 7378–7383.
47. See Supporting Information for details.
48. Rathmell, A. R.; Bergin, S. M.; Hua, Y. L.; Li, Z. Y.; Wiley, B. J. The Growth Mechanism of Copper Nanowires and Their Properties in Flexible, Transparent Conducting Films. *Adv. Mater.* **2010**, *22*, 3558–3563.
49. Chen, J. Y.; Herricks, T.; Geissler, M.; Xia, Y. N. Single-Crystal Nanowires of Platinum Can Be Synthesized by Controlling the Reaction Rate of a Polyol Process. *J. Am. Chem. Soc.* **2004**, *126*, 10854–10855.
50. Carbó-Argibay, E.; Rodríguez-González, B.; Gómez-Graña, S.; Guerrero-Martínez, A.; Pastoriza-Santos, I.; Pérez-Juste, J.; Liz-Marzán, L. M. The Crystalline Structure of Gold Nanorods Revisited: Evidence for Higher-Index Lateral Facets. *Angew. Chem., Int. Ed.* **2010**, *49*, 9397–9400.
51. Katz-Boon, H.; Rossouw, C. J.; Weyland, M.; Funston, A. M.; Mulvaney, P.; Etheridge, J. Three-Dimensional Morphology and Crystallography of Gold Nanorods. *Nano Lett.* **2011**, *11*, 273–278.
52. Brust, M.; Walker, M.; Bethell, D.; Schiffrin, D. J.; Whyman, R. Synthesis of Thiol-Derivatised Gold Nanoparticles in a Two-Phase Liquid−Liquid System. *J. Chem. Soc., Chem. Commun.* **1994**, *0*, 801–802.
53. Khanal, B. P.; Zubarev, E. R. Polymer-Functionalized Platinum-on-Gold Bimetallic Nanorods. *Angew. Chem., Int. Ed.* **2009**, *48*, 6888–6891.
54. Feng, Y.; He, J.; Wang, H.; Tay, Y. Y.; Sun, H.; Zhu, L.; Chen, H. An Unconventional Role Ofligand in Continuously Tuning of Metal−Metal Interfacial Strain. *J. Am. Chem. Soc.* **2012**, *134*, 2004–2007.
55. Feng, Y.; Wang, Y.; Wang, H.; Chen, T.; Tay, Y. Y.; Yao, L.; Yan, Q.; Li, S.; Chen, H. Engineering "Hot" Nanoparticles for Surface-Enhanced Raman Scattering by Embedding Reporter Molecules in Metal Layers. *Small* **2012**, *8*, 246–251.
56. Frens, G. Controlled Nucleation for the Regulation of the Particle Size in Monodisperse Gold Suspensions. *Nat. Phys. Sci.* **1973**, *241*, 20–22.
57. Chen, T.; Chen, G.; Xing, S.; Wu, T.; Chen, H. Scalable Routes to Janus Au−SiO_2 and Ternary Ag−Au−SiO_2 Nanoparticles. *Chem. Mater.* **2010**, *22*, 3826–3828.